EUROPEAN FUSION DEVELOPMENT AGREEMENT

EFDA–JET–PR(05)49

A. Marinoni, P. Mantica, D. Van Eester, F. Imbeaux, M. Mantsinen, N. Hawkes
E. Joffrin, V. Kiptily, S.D. Pinches, A. Salmi, S. Sharapov, I. Voitsekhovitch,
P de Vries, K.D. Zastrow and JET EFDA contributors

Analysis and Modelling of Power Modulation Experiments in JET Plasmas with Internal Transport Barriers

Analysis and Modelling of Power Modulation Experiments in JET Plasmas with Internal Transport Barriers

A. Marinoni[1,9], P. Mantica[2], D. Van Eester[3], F. Imbeaux[4], M. Mantsinen[5], N. Hawkes[6], E. Joffrin[4], V. Kiptily[6], S.D. Pinches[7], A. Salmi[5], S. Sharapov[6], I. Voitsekhovitch[6], P de Vries[8], K.D. Zastrow[6] and JET EFDA contributors*

[1]Politecnico di Milano, dipartimento di Ingegneria Nucleare, Milano, Italy
[2]Istituto di Fisica del Plasma, Euratom-ENEA-CNR Association, Milan, Italy
[3]LPP-ERM/KMS, Association EURATOM-Belgian State, TEC, B-1000 Brussels, Belgium
[4]Association Euratom-CEA, CEA Cadarache, St Paul lez Durance Cedex, France
[5]Helsinki Univ. of technology, Association Euratom-Tekes, P.O.Box 2200, Finland
[6]EURATOM/UKAEA Fusion Association, Culham Science Centre, Abingdon, OX14 3DB, UK
[7]Max Plank Institut fur Plasmaphysik, Euratom Association, Garching, Germany
[8]FOM Institut voor Plasmafysica, Association Euratom-FOM, Nieuwegein, The Netherlands
[9]Ecole Polytechnique Fédérale de Lausanne (EPFL),Centre de Recherches en Physique des Plasmas, Association Euratom-Confédération Suisse, CH 1015, Lausanne, Switzerland
** See annex of J. Pamela et al, "Overview of JET Results ", (Proc. 20th IAEA Fusion Energy Conference, Vilamoura, Portugal (2004)).*

Preprint of Paper to be submitted for publication in
Plasma Physics and Controlled Fusion

"This document is intended for publication in the open literature. It is made available on the understanding that it may not be further circulated and extracts or references may not be published prior to publication of the original when applicable, or without the consent of the Publications Officer, EFDA, Culham Science Centre, Abingdon, Oxon, OX14 3DB, UK."

"Enquiries about Copyright and reproduction should be addressed to the Publications Officer, EFDA, Culham Science Centre, Abingdon, Oxon, OX14 3DB, UK."

ABSTRACT

Understanding the physics of Internal Transport Barriers (ITBs) is a crucial issue in developing ITER relevant advanced tokamak scenarios. To gain new information on ITBs, RF power modulation experiments, mainly devoted to the study of electron heat transport through ITBs, have been performed on the JET tokamak. The main physics results have been reported in [1]. The present paper describes in detail the data analysis and numerical modelling work carried out for the interpretation of the experiments. ITBs located in the negative shear region behave as localized insulating layers able to stop the heat wave propagation, thus implying that the ITB is a region of low diffusivity characterized by a loss of stiffness. Various sources of spurious effects affecting the interpretation of the results are analysed and discussed. Empirical transport models have been set up and satisfactorily reproduce the data, but first principle based models have so far failed to predict the temperature profile in first place, which prevented their application to modulation results.

1. INTRODUCTION

Power modulation experiments allow to perform heat transport studies in a medium by following the heat pulse propagation at various frequencies, thus allowing to estimate the conduction and convection contribution to the total heat transport [2].

In the past these techniques have been widely applied to L and H mode plasmas [3, 4] in order to investigate electron heat transport. Only recently similar experiments have been performed in JET plasmas characterized by strong and long lasting Internal Transport Barriers (ITBs). This paper describes in more detail the methods of analysis and the modelling work that are at the basis of the interpretation of the results described in [1].

There are still several questions about the basic physics governing transport in ITB regions, among these: is an ITB a spatially localized layer or a wide core region? Which transport mechanisms are acting within the ITB? Which is the type of transition mechanism that induces the ITB formation? Power modulation experiments performed in JET ITB plasmas in order to explore electron transport through them allow to address some of the above issues with non-standard tools. Perturbative experiments are extremely powerful in highlighting peculiarities that are simply not visible in a standard power balance analysis, thus setting a set of constraints which are able to provide a more complete view of the transport processes.

The present paper is organized as follows: Sect.2, contains a description of the experimental set up and a summary of the main experimental results, Sect.3 describes the methods of analysis of experimental data, Sect.4 concerns numerical simulations aiming at deriving a diffusion coefficient which is able to describe experimental data, in detail, reproducing all their peculiarities, Sect.5 summarizes the conclusions.

2. OVERVIEW OF EXPERIMENTAL RESULTS

2.1.EXPERIMENTAL SET-UP

The modulated power source used was Ion Cyclotron Resonance Heating in the Mode Conversion [4,5] (MC) scheme. Despite the lack of an Electron Cyclotron Resonance Heating at JET, a direct and localized power to electrons, suitable for transport studies, is indeed achievable on JET using ICRH.

The chosen minority specie was He^3, in D plasmas, at concentrations, regulated via a real time control, ranging from 10% to 20% with respect to electrons. At these concentrations a significant fraction (from 30 to 50%) of the RF power is converted into a short wavelength bernstein wave at the Ion-Ion-Hybrid (IIH) layer and directly absorbed by electrons. The deposition location depends upon magnetic field, RF frequency and the minority concentration[4]. In fusion machines the presence of He^3 will allow to increase fusion performances, here it merely serves to ensure a direct electron heating.

Plasmas are characterized by a flat top current of 2.6-2.8MA, a line averaged electron density of $2\text{-}3\times10^{19}$ m^{-3}, elongation around 1.75, up-down averaged triangularity of about 0.25 and 3.25-3.6 T as toroidal field on the magnetic axis. Lower Hybrid preheat of 2MW has been applied in order to get a deeply reversed q profile. 13-18MW NBI extra power was also supplied to sustain the barriers, while the RF power was on average 4MW with a half depth modulation characterized by a duty cycle of 0.6 and a modulation frequency ranging from 4 to 45Hz. The phasing of the RF has been almost always set to $-\pi/2$ due to its better performances compared to other phasings, since it minimizes ion damping in presence of co-injected NBI ions[4].

The Electron temperature is measured by the Electron Cyclotron Emission (ECE) diagnostic which, at JET, has 96 channels and is characterized by a radial uncertainty of about 3cm (3% of the minor radius) and by an acquisition frequency up to 3kHz along a line of sight located about 13cm below the $Z=0$ axis of the vacuum vessel. The analysis concerns only electrons since Charge Exchange Recombination Spectroscopy (CXRS) diagnostic does not allow perturbative studies of ion transport due to its lower acquisition rate compared to the RF power modulation frequency.

2.2. RESULTS

Two power deposition schemes, characterized by two different minority concentrations, have been used, the first one at about 10-12%, which we will refer to in the following as C12, and at about 20%, the C20 regime. The reason for this distinction lies in the amount of power that is effectively coupled to electrons, at the IIH resonance layer. As the minority concentration raises, there are two competing effects taking place: the first one is given by a larger amount of mode converted power due to an increased distance between the fundamental He^3 ion cyclotron resonance and the MC layers, the second one is an increase of the amount of the RF power that is transferred to NBI fast ions [4]. This results, with respect to the quantity of power coupled to electron, in an optimum concentration of minority species in the plasma which has been estimated, via numerical simulations

fitting experimental data, in 18-20%; this is in accordance with results of previous experiments in L and H mode plasmas [2].

Regarding plasma performances the first scenario gave the best results achieving central electron density of 5×10^{19} m^{-3}, total energy confinement times up to 0.5s, electron and ion temperatures of 13 and 24keV respectively. In Figure1 a comparison of two typical cases, belonging to C12 and C20 respectively, is shown.

The goal of the experiment is to deposit the MC power at a given distance from the ITB, then to study the propagation of the resulting heat wave across it. In this regard, two experimental configurations have been achieved: in the first one the MC power is deposited on the barrier, while in the second one it is shifted on the high field side with respect to it. In the first case the heat wave is rapidly and completely damped in the ITB region and cannot leave it, while in the second one there is at least one, sometimes two, depending on the particular configuration, heat waves which travel suffering almost no damping in the turbulent plasma up to the ITB, where they are quenched. The second heat wave present in some cases is given by Fast Wave Electron Landau Damping (FW-ELD) and Transit Time Magnetic Pump (FW-TTMP) processes, which yield a direct electron power deposition on-axis. The occasional absence of this central peak is due to the amount of power effectively converted, to its profile and to the ECE line of sight which, since it does not pass through the magnetic axis, might not be able to see the peak.

The basic idea which lies behind modulation studies is to perturb periodically the injected power, and then to study the fourier expansion of the electron temperature perturbation which is a response to the power modulation; depending upon the amount of power deposited, it presents a higher or lower amplitude of oscillation. In this way it is possible to observe the deposition and the propagation of the heat wave by calculating the amplitudes and the phases of the expansion serie by standard FFT techniques, applying an hanning window, or the amplitude coefficients using the Break In Slope (BIS) [7] analysis. The region where the maximum of the modulated power is deposited, presents the highest modulation amplitude and the lowest value of the phase. This statement can be understood by looking at the very simple model of Equations (1), which take into account a constant diffusion coefficient with no convection. Equation 1b is obtained developing to first order Equation 1a in the perturbed quantities indicated by tilde superscripts.

$$\frac{3}{2} n_e \frac{\partial T}{\partial t} - n_e \chi \nabla^2 T = P_{rf} + P_{ohm} + P_{ei} \tag{1a}$$

$$\frac{3}{2} n_e \frac{\partial \tilde{T}}{\partial t} = \chi\, n_e \frac{\partial^2 \tilde{T}}{\partial x^2} + \frac{\partial P_{ohm}}{\partial T} \tilde{T} + \frac{\partial P_{ei}}{\partial T} \tilde{T} + \tilde{P}_{rf} \tag{1b}$$

In Figure 2 we present a typical example of ECE time traces and, in Figures 3 the resulting FFT for the two cases afore mentioned.

The whole analysis focused only on ECE data for which the spectrum shows a clear peak at the modulation frequency well above the noise level.

In Figures 3b-d-e error bars are estimated performing a simulation which takes into account a white noise characterized by a standard deviation equal to the ECE data one of these two shots, a time step equal to ECE acquisition rate, and a number of points equal to the experimental one. These estimated error bars give an approximate idea of the uncertainty level in these FFT analyses, i.e. 5-15%. They will not be shown in the following graphs.

One debated question about the physics of the ITBs is if they are regions of stiff transport with a higher threshold rather than regions where turbulence is suppressed. In order to answer this question one should estimate if the incremental diffusivity

$$\chi^{inc} = \chi_0 + \frac{\partial \chi}{\partial \nabla T} \nabla T \tag{2}$$

is very high or not. In the first case one would have to observe heat waves propagating across the ITB with a small attenuation depending upon the stiffness level, while in the second one the heat wave is completely damped. Our experimental observations led us to be inclined towards the second hypothesis since, as shown in Figures 3(d-e), the heat wave is rapidly damped in the ITB region. In Figure 3(b), where the power is deposited on the barrier, the heat wave cannot leave it, while in the second case, the two waves, MC and the one generated by FW-ELD+FW-TTMP processes, are both quenched by the barrier. The sharp changes in the values of amplitude and phase in Figure 3(d) should be compared to the ones in Figure 3(e), which refers to the same pulse but in a phase without ITB.

Another basic question about ITBs is whether they are the result of a general improvement of the confinement in the whole core region or rather if they are just a layer, characterized by a low conductivity, embedded in a more turbulent plasma. Looking at Figure 3(d), where the heat waves are deposited outside the barrier, it is seen that the heat wave due to FW-ELD+FW-TTMP travels from the very centre to the ITB, where it is damped. This suggests, in accordance with numerical simulations discussed in the next section, that the second hypothesis is closer to reality. In fact, if the contrary was true, the central heat wave would have to be quenched by the low conductivity region between the magnetic axis and the ITB. We note that in Figure 3d the amplitude at the inner inside of the ITB does not start decreasing exactly where the phase rises probably due to the presence of the weak minority peak (phases do not show a minimum due either to the delay induced by collisional processes, which raises the phase values to a level comparable to the ones of waves propagating from the FW and MC resonances, or to the small amplitude of the deposited power).

Looking at the slopes of the amplitude in Figure 3d one could also deduce that the values of the diffusion coefficient are higher in the outer part of the ITB with respect to the inner part; as can be formally inferred by means of the following formula valid in cylindrical geometry without taking into account a heat pinch velocity [2] (where χ is the diffusion coefficient, A the amplitude, φ the phase, ω is 2π times the perturbation frequency, r the minor radius and the symbol prime means radial derivative)

$$\chi = \frac{3}{2} \frac{\omega}{\varphi^2 \left(\frac{A'}{A} + \frac{1}{2r} - \frac{\nabla n}{2n} \right)} \tag{3}$$

This basically means that the ITB could be not characterized by a uniform configuration and that the turbulence stabilization would be stronger closer to the magnetic axis which, by the way, would be consistent with an enhanced value of the negative magnetic shear.

3. DATA ANALYSIS

3.1. DETERMINATION OF HE³ CONCENTRATION AND RF POWER DEPOSITION

The position of the MC layer, at which the dominant electron damping occurs in the MC regime, is a function of the magnetic field, of the RF frequency and of the minority concentration; as a general rule it shifts towards the high field side with decreasing magnetic field strength and with increasing minority concentration. Thus, in order to keep the position of the IIH resonance layer as constant as possible (to have a fixed power source), a Real Time Control (RTC) of the helium concentration has been developed. By writing the equations of quasi-neutrality and the definition of Z effective

$$\begin{aligned} 1 &= \sum_i Z_i \, \xi_i \\ Z_{eff} &= \sum_i Z_i^2 \xi_i \end{aligned} \tag{4}$$

where the index spans all the ion species present in the plasma, the minority concentration can be controlled in real time if the ratio of the deuterium concentration and of the various impurities under consideration is monitored, for example, using the divertor light. In fact if, for the sake of semplicity, one considers only carbon as relevant impurity, combining the two Equation (4) one gets

$$\xi_{He^3} = \frac{6 - Z_{eff}}{8 + 5 \frac{\xi_D}{\xi_{He^3}}} \tag{5}$$

where the divertor light is used to estimate the ratio between deuterium and He^3 densities.

This method holds rigorously only for the edge of the plasma, while for the centre two other diagnostics, which do not possess the properties to be used in the RTC, have been used. The first one is the CXRS which provides the densities of light impurities, such as C Li Be, over the whole plasma radius. The second one employs the production of gamma rays in the following reaction

$$He^3 + \mathrm{D} \rightarrow L_i^5 + \gamma + 17 MeV \tag{6}$$

In two twin pulses, i.e. with quite the same characteristics, a difference in the production rate of gamma rays strongly suggests a difference in the RF heated minority concentration. In fact, as far as the mode converted power increases with the minority concentration, i.e. when the latter is lower than 18- 20%, the more minority ions are present, the more power goes to electrons via MC

phenomenon. Now, for a given RF and NBI power deposition, the higher the energy of fast ions, the lower the concentration of the concerned minority specie and thus the amount of power converted. At high minority concentrations this reasoning fails.

The NBI power deposition is estimated using the code PENCIL, the RF heating one via PION[8] and TOMCAT[9] simulations. The latter is cross-checked with experimental estimates of power absorption using both the BIS method and the analysis of high frequency modulation components [10]. At concentrations ~12% and for the high temperature of the type of shot shown in Figure 2, about 30-40% of the RF power is directly absorbed by the electrons in the MC region while only a small amount is directly absorbed on the fast wave. Although central minority ion heating is still high (>=50%) at this He^3 level, a highly energetic He^3 tail can no longer be formed so the power is mainly transferred to bulk ions, leaving MC as the only source of modulated electron heating. At concentrations ~20%, for the type of shot shown in Figure 4, ion heating is less significant and about 80% of the power is absorbed by the electrons, half via MC at the IIH layer with a localized profile, half in the centre via ELD+TTMP processes. In both cases the modulated electron source term due to collisional coupling with ions has been estimated by simulations to be completely negligible(<2%) with respect to the RF modulated source, due to the small amplitude of both T_e and T_i perturbations (<100eV)

In Figure 3 we show all the power deposition profiles for Pulse No: 59397 at 6.5s.; the width of the MC profile, in this case of on-ITB deposition, is remarkably narrow thus leading to a very localized power deposition.

3.2. THE IMPACT OF MHD ACTIVITY ON HEAT WAVE ANALYSIS

Theoretical analysis of the resulting FFT coefficients[2,11,12] give precise constraints on amplitude and phase values (when they refer to a reference value, such as the phase of the input power), here it is enough to say that there must be a regular trend of phases and amplitudes of the various harmonics; thus we kept in the analysis the first three coefficients because, in general, they are enough to verify the theory and not too much affected by noise. In the following we consider only pulses with peaks at the modulation frequency much higher than the average noise level; the reason for this will be immediately clarified in the following.

As the concerned plasmas are characterized by huge gradients, e.g. 0.5keV/cm on average in the barrier region, they are subject to MHD instabilities. Identified as internal kink modes with n=1 and an even value of m (probably 2), these instabilities redistribute very quickly heat and particles around an inversion radius thus polluting the electron response to power modulation (see for example Figure 2). The resulting power spectra present peaks at several harmonics located at the position of the ITB. Therefore it is necessary to perform FFT analysis in between crashes since these can invalidate the results, as shown in Figures 5. In this figure we also note how MHD instabilities are able to produce peaks at higher harmonics, when in reality these are due to noise, referring to the modulation issue.

Since the quality of the FFT increases with the number of samples retained in the analysis, MHD instabilities cause a serious loss of data which can be analysed, if they happen too frequently.

3.3. RELATION BETWEEN Q PROFILE AND ITB LOCATION

Theoretically the magnetic configuration plays a crucial role in the stabilization of turbulence[13], thus enabling the formation of an ITB. It is to be noted however that there is still discussion about the role played by rational values of the q profile[14]. Unfortunately an accurate reconstruction of the internal magnetic configuration is not always available; in these experiments it is performed by the code EFIT [15] with Motional Stark Effect (MSE) constraints [16].

In Figure 7a the q profile level lines are shown together with the electron temperature gradient as a function of time and major radius. In order to verify the accurateness of the q profile we cross-checked it with Alfven Cascades [16] diagnostic (AC), that give the time at which a rational q minimum appears in the plasma, and with a localization of MHD instabilities, obtained by computing the coherence between magnetic and ECE signals. In fact it is possible to determine, at least, if the MHD instability is localized on a magnetic surface which has an even or an odd value of m; usually the n value is known. The typical uncertainty on the position of the modes, and so on the rational magnetic surface, is about 15cm, which is 15% of the minor radius (Figure 6).

From Figure 7(a) it is evident that the ITB lies in the region of negative magnetic shear and, looking at the neutron flux and at temperature and density time traces, according also to AC data, we notice a temporal coincidence between the rational q minimum arrival time and a strengthening of the barriers, in agreement with a number of previous observations [18,19] (Figure 7(a-b)). Figure 7a would suggest that the foot of the barrier lies where the q minimum is and that the ITB moves in the region of negative magnetic shear after being born on the minimum of the safety factor. We remind, however, that MSE error bars yield an uncertainty on the q profile of up to 5cm in the radial direction.

3.4. ANALYSIS OF FUSION PERFORMANCE

Pulse Number 59411 has been simulated with the TRANSP code [20] in order to evaluate its equivalent fusion performance Q_{DT} for a bulk ion composed of 50% D and 50% T. To best reproduce the experimental neutron flux, the distribution of light impurities was taken from CXRS measurements, while for heavy impurities, for which only a line integrated measure exists, an off-axis distribution was required. The estimated triple product is 10^{20} keV s m^{-3}, and the equivalent Q_{DT} is approximately equal to 0.23. This value, despite being pretty lower than one, represents one of the best results obtained by a deeply reversed shear ITB dicharge on the JET tokamak.

Q_{DT} is calculated as $P_{out}/(P_{in}\text{-}dW/dt)$, where W is the plasma diamagnetic energy, P_{in} is the total injected power which is the sum of ohmic, neutral beam, ICRH powers and P_{out} is the actual fusion power, calculated as the fusion rates of DD-DT-TT, of which the most important is by far the DT, times the energy produced in each reaction (e.g. 17.6MeV for the DT one; fusion processes considered

are beam-beam, beam-bulk and bulk-bulk). Since it is not known if, in order to have the same profiles, the input power from NBI or ICRH could be replaced by the alpha particle power, the latter is summed in the numerator of the equation and not subtracted in the denominator.

4. NUMERICAL MODELLING

4.1. SPURIOUS EFFECTS

Before simulating experimental results one, of course, has to be sure that they are not a consequence of any spurious effect. The first indication, in modulation experiments, is to look at the power spectrum of the data and be sure that the peaks at the modulation frequencies are well above the noise level.

There are however various effects that can affect the spectral response or even introduce peaks well above noise in the spectrum which do not result from propagation of the heat wave generated by power modulation

One possible effect, as described in the last section (Figures 5(a-b)), is the presence of MHD crashes which could have a frequency component at the modulation frequency. Others could be a modulated plasma displacement and a modulation of the χ profile due to the modulated RF power. The first effect exists because the ECE diagnostic measures plasma temperature at an almost fixed position given mainly by the toroidal magnetic field; so if the plasma moves as a rigid body in the laboratory reference frame, ECE will sample the temperature of different radial points of the plasma thus producing a spurious modulation which will grow in magnitude with the temperature gradient and with the amount of displacement. Such an effect should produce a π phase shift in the FFT performed at the high field side with respect to the low field side since the temperature radial gradient has opposite directions at the high field side and at the low field side. Experimentally this is not the case, as shown in Figure 10.

Moreover this effect has been also simulated using the code CRONOS [22], which has an easy way to express profiles in the laboratory reference frame, which is the one of ECE, and in the plasma one, which is the reference frame where transport studies have to be carried out. Figure 11 shows the difference between the results in the two afore mentioned frames; being it up to 10-15eV, is not responsible for the observed peak at the ITB. In addition the difference is an effect which is fairly uniform on the whole barrier and does not even reproduce a peak.

The second effect has been simulated using the code ASTRA [23] assuming a parabolic χ profile with a hole that allows to reproduce the ITB. The depth and the width of the hole, or part of them, have been modulated in different ways, with or without phase differences with respect to one another, but no satisfactory agreement with the experiments has been found; in Figure 12 we show just an example. In this figure the existence of two peaks is due to the modulation of the χ profile which induces, mainly, a modulation of the temperature gradient in the barrier region; this, in turn, results in a modulation of the electron temperature whose highest values are at the borders of the barrier.

4.2. MODELLING USING SEMI-EMPIRICAL MODELS

The use of empirical transport models with parameters that are adjusted in order to achieve good reproduction of the data provides a tool to get insight into the mechanisms at work in the plasma and to test basic physics idea, even if such models are not derived from 1st principle theories.

4.2.1. Constant χ_e model

The first model is a simple parabolic χ profile, with a depression at the ITB location (Figure 13a), which allows a good reproduction of the temperature profile and the amplitude of all the first three harmonics, but the reproduced phases are too low compared to the experimental ones.

Concerning the power radial profiles inserted into the simulations, the mode converted power is much narrower than all the others, as shown in
Figure 3, when the power is deposited on the barrier; while when the IIH layer is far away from the ITB its width is about three times larger, which is a value consistent with previous experiments in L and H mode plasmas[3].

Moreover, as anticipated in the previous section, we studied a variant of this model presenting a very low χ profile in the whole region, for both configurations, bounded by the ITB; this model did not allow to reproduce the electron temperature profile in a consistent way with experimental data. In fact, besides failing in reproducing the afore-mentioned change in the slopes of amplitude and phases profiles at the ITB location, in order to get a fitting simulated temperature it has been necessary to artificially take out almost all the power coupled in the centre of the plasma via FW ELD-TTMP.

4.2.2 Critical Gradient Model

This model is an adaptation of the critical gradient model[13]. The adopted diffusion coefficient is given by

$$\chi_e = \chi_s p^\nu \frac{T_e}{eB}\frac{\rho_s}{R}\left(\frac{-R\partial_r T_e}{T_e} - k_c\right) H\left(\frac{-R\partial_r T_e}{T_e} - k_c\right) + \chi_s p^\nu \frac{T_e}{eB}\frac{\rho_s}{R} \tag{7}$$

where p is an increasing function of the radius, B the magnetic field, $\rho_s = \sqrt{(m_i T_e)}/eB$, H is the heaviside function, k_c is the threshold and the parameters ν χ_0 and χ_s have been set using the simulation in order to get the best match with experimental data.

Using the same power deposition profile of the previous model, the best reproduction has been obtained setting the ITB region under threshold but, as illustrated in Figures 14 even though we got a fairly good reproduction of the amplitudes and temperature profiles, phases are still too low.
The situation gets better considering the simulation of Pulse No: 62077, characterized by MC power deposition outside the barrier, as illustrated in Figures 14(e-f).

The extremely high value of the phases does not characterize all the pulses with MC deposited on the barrier, but seems to have a modulation frequency dependence; in fact if this last one is increased by a factor 3, it is indeed possible to simulate well also the phases, as shown in Figure 15.

4.3. MODELLING USING FIRST PRINCIPLE MODELS

Although unfortunately, due to the long period of the simulation, it is not possible to perform 3D fluid turbulence simulations to try reproducing the experimental FT coefficients, still some attempt to compare the data with predictions from first principle1D-averaged fluid turbulence models is in principle possible. Among those available at the moment, we chose to try a simulation using the GLF23 [24] model because it is the only one featuring a significant stabilizing role of a reversed magnetic shear. The model was used as implemented in the ASTRA code. The simulation did not allow us to compare simulated and experimental FT because it did not reproduce the ITB temperature profile in first place (Figure 16), so that any further investigation was useless. One possible reason for the failure of the GLF simulation, which does not seem to depend neither on Z_{eff} nor on s/q, might be the lack of experimental information about poloidal velocity whose neoclassical value [25], set in the simulation, may not be appropriate in high power NBI pulses (considering also that the MC is expected to drive a sheared poloidal flow [26]). More studies of this kind are clearly required, especially by benchmarking the same model implemented in different codes and used in plasmas of different tokamaks. Such a study has been attempted in [27], where similar conclusions, with respect to the GLF23 predictive simulation presented here, have been reached.

CONCLUSIONS

Experiments of power modulation aimed at studying electron heat transport through ITBs have been performed at JET using the Mode Conversion scheme, with Real Time Control of the He^3 concentration. Results are pretty encouraging regarding plasma performances with electron and ion temperatures up to 13 and 25keV respectively, while the electron density reaches 5×10^{19} m^{-3}. The ITBs were located in the negative magnetic shear region.

The ITB behaves like an insulating layer, very localised in space, which is able to damp all the heat waves that cross it. This implies that the barrier is a region of low diffusivity characterized by a loss of stiffness. By comparing the damping factors of the heat waves crossing the ITB region, first experimental results may indicate a non-uniform radial configuration of the barrier, characterized by a higher stabilization of the anomalous transport in its inner part with respect to the outer one. Various sources of spurious effects affecting the heat wave propagation results have been examined. The data can be reasonably reproduced with numerical simulations using empirical models describing the barrier as a region of reduced diffusivity, while all the surrounding plasma is characterized by a higher level of transport. However first attempts to use first principle models did not succeed in reproducing the ITB itself, so no test on the heat wave propagation data was possible.

ACKNOWLEDGEMENTS

We thank Drs. X.Garbet, A.Thyagaraya, C.Angioni and R.Cohelo for useful discussions. This work has been conducted under the European Fusion Development Agreement.

REFERENCES

[1]. Mantica P et al., "Probing internal transport barriers with heat pulses in JET", accepted by *Phys. Rev. Lett.*

[2]. Jacchia S et al., *Phys. of Fluids* **B 3**, 3033 (1991)

[3]. Mantica P et al., *Plasma Phys. Contr. Fusion* **44**, 2185 (2002)

[4]. Mantsinen M et al., *Nucl. Fusion* **44**, 33 (2004)

[5]. Stix T H, Waves in plasmas (New York: AIP)

[6]. Tresset G, *Nucl. Fusion* **42**, 520 (2002)\

[7]. Van Eester D, 15th Top.Conf. on RF Power in Plasmas, Wynoming, USA (2003), 66

[8]. Eriksson L G et al., *Nucl. Fusion* **33**, 1037 (1993)

[9]. Van Eester D et al., *Nucl. Fusion* **42**, 310 (2002)

[10]. Gambier D J et al., *Nucl. Fusion* **30**, 23 (1990)

[11]. Leuterer F et al., *Nucl. Fusion* **43**, 744 (2003)

[12]. Ryter F et al., *Plasma Phys. Control. Fusion* **43**, A323 (2001)

[13]. Garbet X et. al, *Nucl. Fusion* **43**, 975 (2003)

[14]. Candy J et al., *Phys. of Plasmas* **11**, 5, 1879 (2004)

[15]. Lao L L, *Nucl. Fusion* **30**, 1035 (1990)

[16]. Hawkes N et al., *Rev. Sci. Instr.* **70**, 1 (1999)

[17]. Sharapov S et al., *Physics Letters A*, **289** (2001)

[18]. Joffrin E et al., *Nucl. Fusion* **43**, 10, 1167 (2003)

[19]. Challis C et al., *Plasma Phys. Contr. Fus.* **44**, 1031 (2002)

[20]. http://w3.pppl.gov/transp/

[21]. Welch P D, *IEEE Trans. on Audio and Elec.*, vol. AU-15, 2, 70 (1967)

[22]. Basiuk V et al., *Nucl. Fusion* **43** (2003) 822830

[23]. Pereverzev G et al., IPP report **5**/98 (2002)

[24]. Waltz R E et al., *Phys. of Plasmas* **4**, 2482 (1997)

[25]. Kim Y B et al., *Phys. of Fluids* **B3**, 2050 (1991)

[26]. Jaeger E F et al., *Phys. Rev. Lett.* **90**, 19 (2003)

[27]. Tala T et al., "Fully Predictive Time-Dependent Transport Simulations of ITB Plasmas in JET, JT-60U and DIII-D", to be submitted to *Nuclear Fusion*.

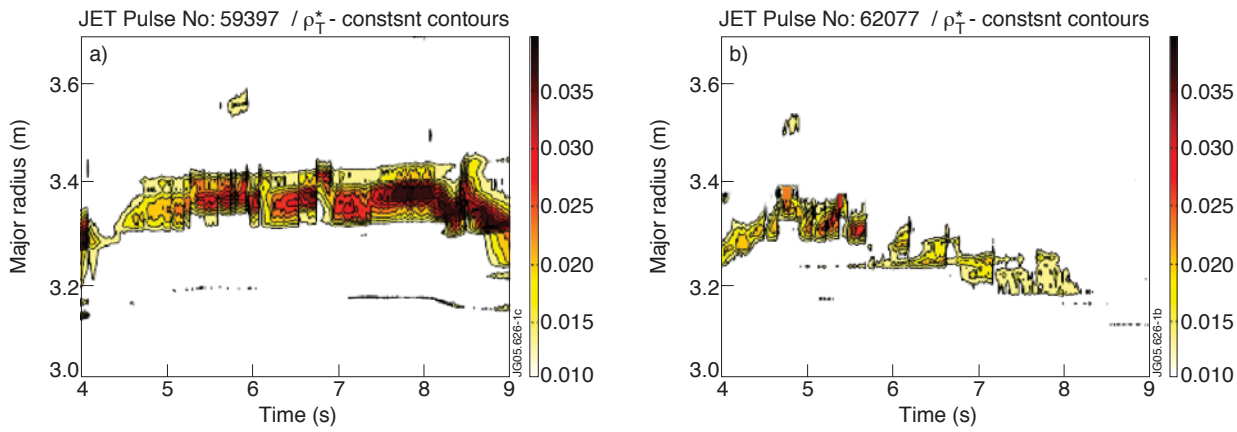

Figure 1: Comparison a C12 shot, on the left, and a C20 one, on the right expressed as Tresset criterion[6]. In the case of C12 the ITB is stronger leading to better fusion performances.

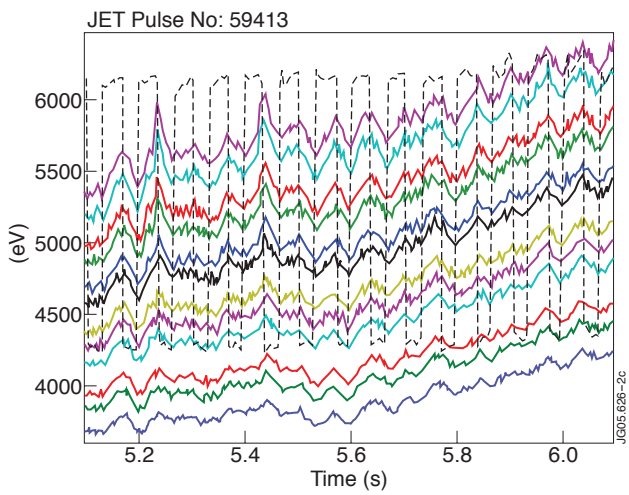

Figure 2: Temporal temperature traces of ECE (full lines, [eV]), and modulation of ICRH antenna(dashed line in arbitrary units). Temperature responds to the input in different places even though some MHD events disturb the modulation.

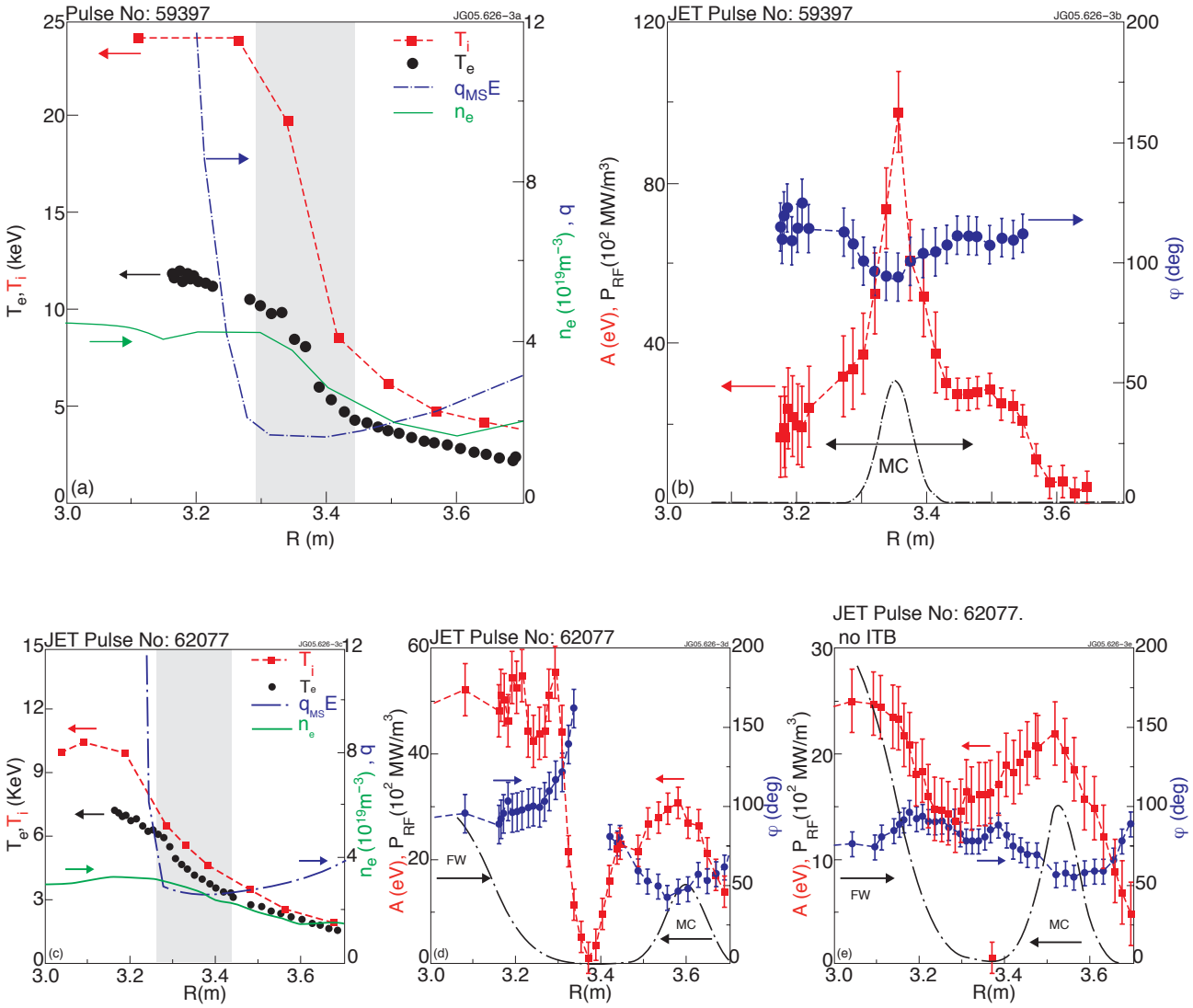

Figure 3 (a,c): (Top,bottom-left).Te(circles) Ti(squares) ne (full line) vs q profile (dashed line) for Pulse No's: 59397 at 5.5s and 62077 at 5.6s respectively.
Figure 3 (b, d, e): Radial profiles of the MC+FW power deposition (dashed), FFT amplitude (squares) and phase (circles) for power deposition on the barrier, outside it and without an ITB. Missing points in the phase profile of Figure 3 (d): are due to extremely large error bars, caused by the low value of the amplitude, which pollute excessively the values.
In Figure 3(b): FFT is performed at time 5.2-5.54s, in d at 5.4-5.7s, in e at 8-9s.

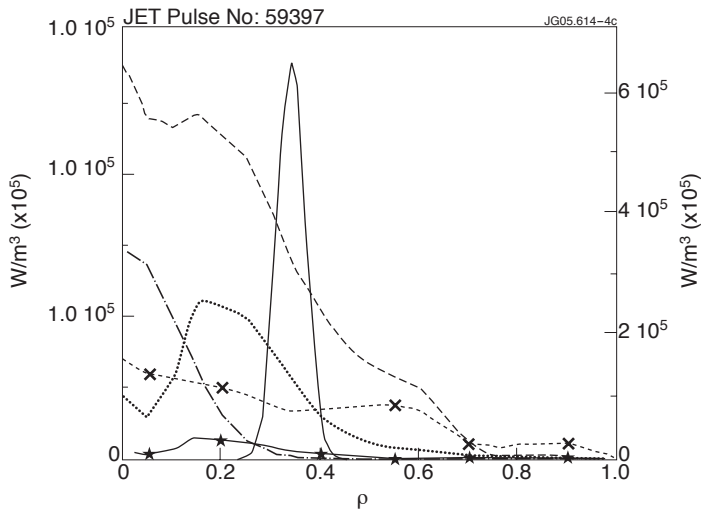

Figure 4: Power deposition profiles, expressed in Wm^{-3}, used in the simulations. On the right scale the NBI transferred to ions (dotted line); on the left the NBI transferred to electrons (dotted line (+)), RF collisional power to ions (dashed line) and to electrons (dashed line(×)) are simulated by PION[8]. MC (full line) and ELD+TTMP (hatched line) are estimated by ASTRA in order to match the experimental profiles of Pulse No: 59397.

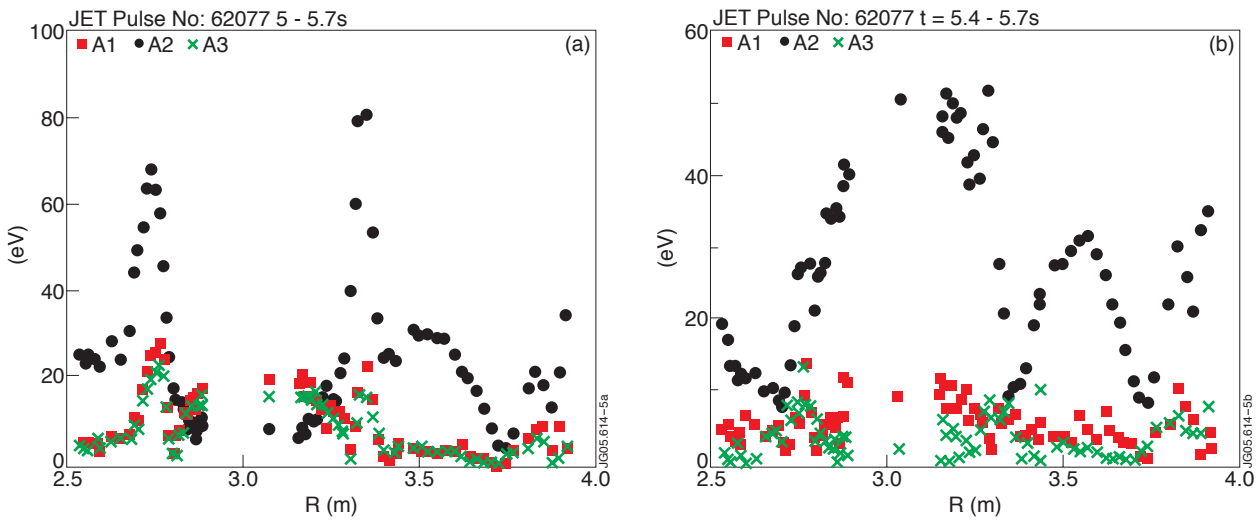

Figure 5: Picture illustrating the difference between performing FFT with (a) and without (b) MHD crashes. The off-axis wide peak is the actual MC power. Here only the first harmonic is sufficiently unpolluted by noise to give appreciable results linked to the modulated RF power.

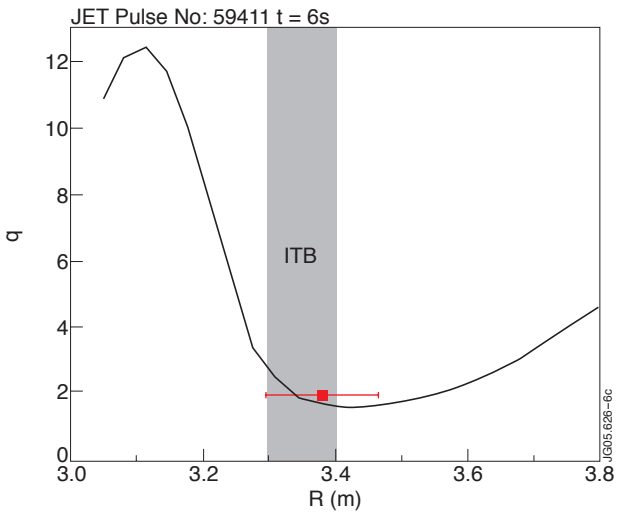

Figure 6: Q profile (circles) versus ITB region and localization of the mode n=1 m=2 (square) with its uncertainty.

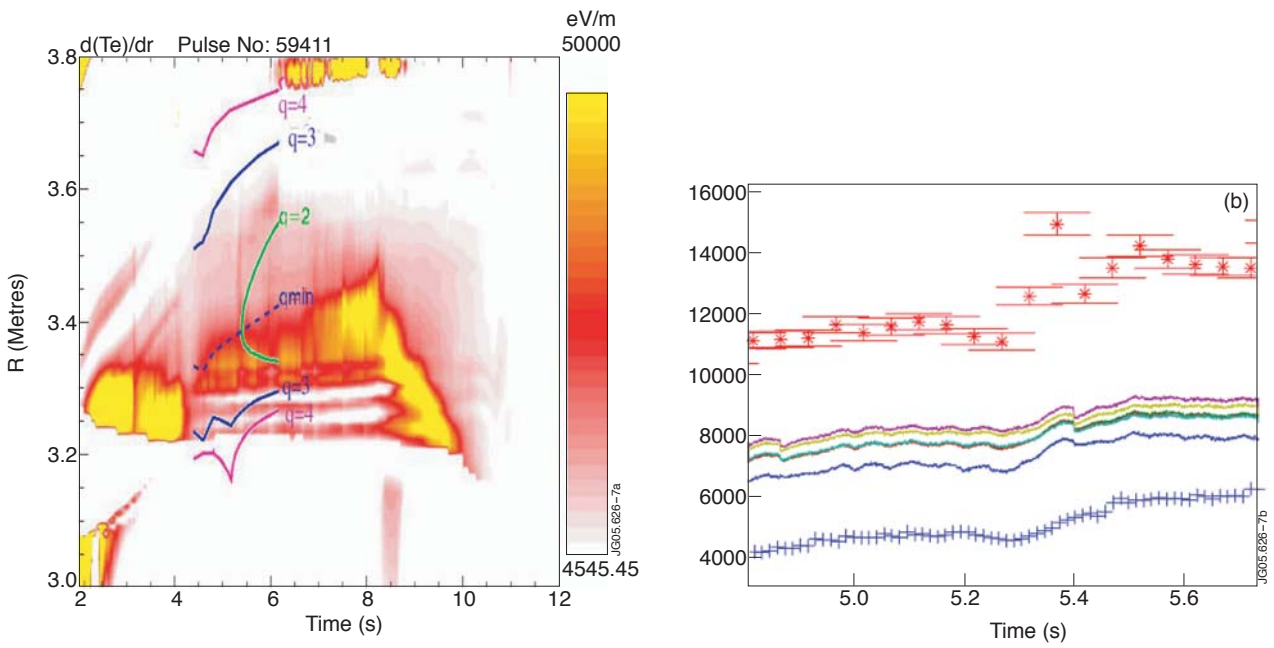

Figure 7 (a): Temporal evolution of the electron temperature radial gradient as a function of the major radius. The level lines of the q profile reconstructed with MSE constraints are superimposed. (b) Temporal evolution of the neutron rate (crosses [1e12/s]), on axis Ti (stars [eV]) and central Te at 6 different points (continuous lines [eV]). The increase in the values is in coincidence with the arrival time of the q minimum surface q=2 provided by AC and MSE diagnostics.

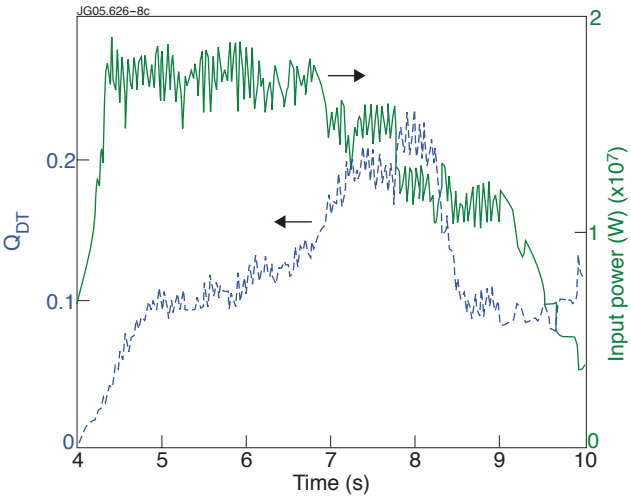

Figure 8: Total input power and calculated equivalent Q_{DT} for Pulse No: 59411. The fast beam ions slowing down time is 0.15s as estimated from the PENCIL code over the hole time scale.

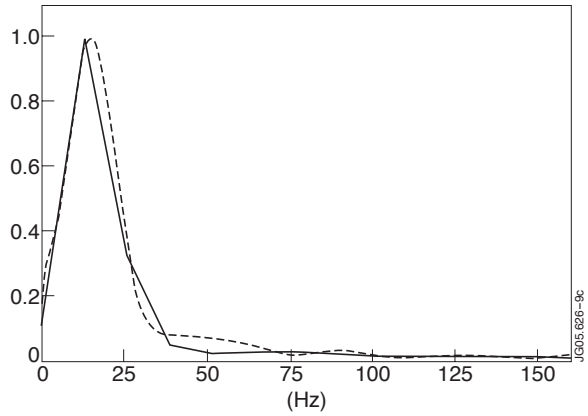

Figure 9: Power spectral density (in arbitrary units) of an ECE channel corresponding to the barrier region (full line), and of the input RF power (dashed line) for Pulse No: 59397, calculated via the Welch averaged periodgrams method [21].

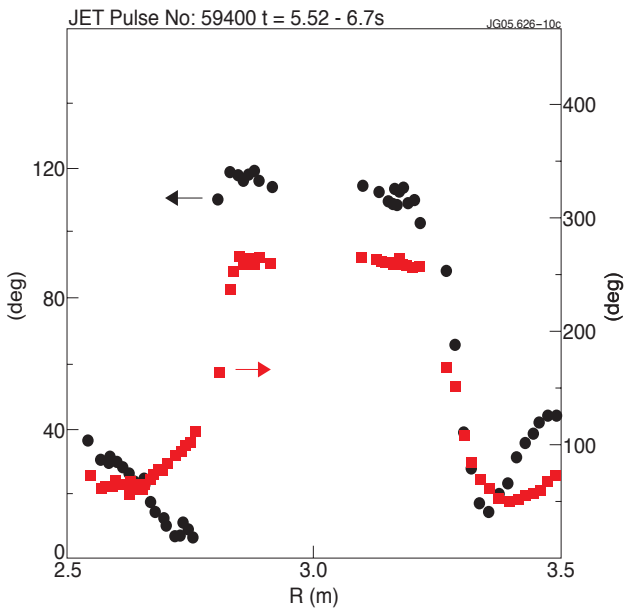

Figure 10: Phases, expressed in degrees, of the first two harmonics for Pulse No: 59400. The symmetry of high and low field sides assures that the peaks are not due to a rigid displacement of the plasma. Minima indicate that power is actually deposited in the region. The different slopes around each minimum illustrate different values of the χ profile, that is lower for steeper curves.

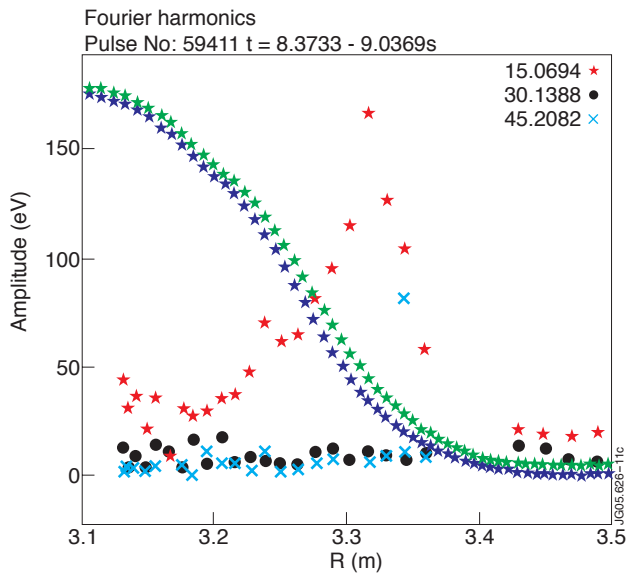

Figure 11: Comparison of first harmonic experimental amplitude (red stars) with first harmonic simulated one in the plasma reference frame (blue stars) and in the laboratory one (green stars). In this simulation the power has been put on the magnetic axis, but the situation does not change significantly if it is placed on the ITB. Light blue circles and green crosses represent experimental second and third harmonic amplitude respectively.

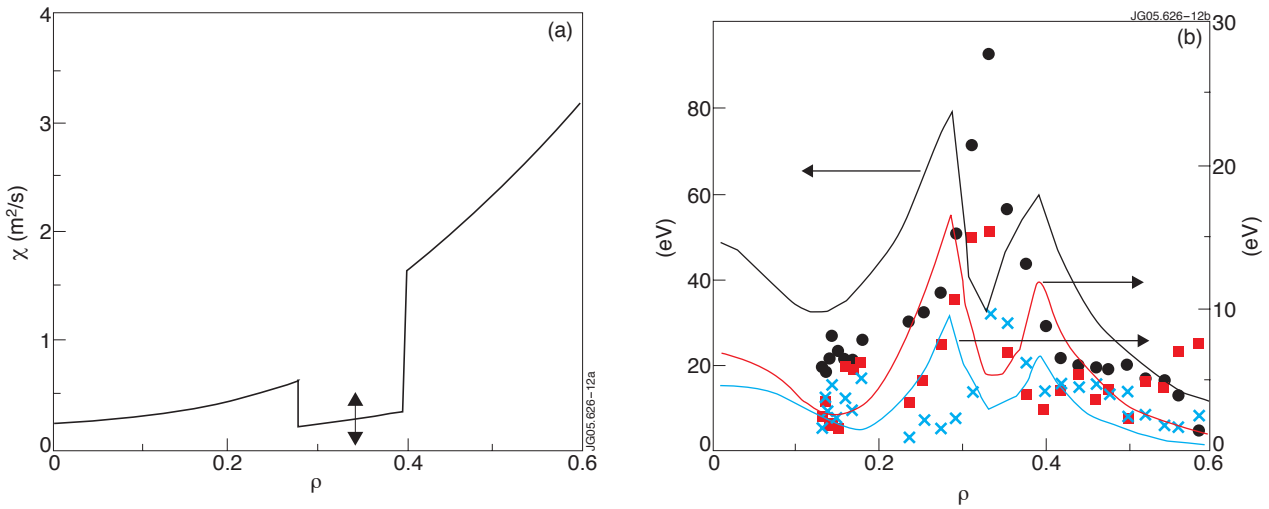

Figure 12 (a): C profile used in the simulation as a function of the normalized squared root of the toroidal flux. (b) Effect of the modulation of the bottom of the hole of the χ profile on amplitudes coefficients versus experimental ones for the first three harmonics. First harmonic (left scale) is represented by circles versus full line, the second one (right scale) by squares versus dashed line, the third one (right scale) by crosses versus points.

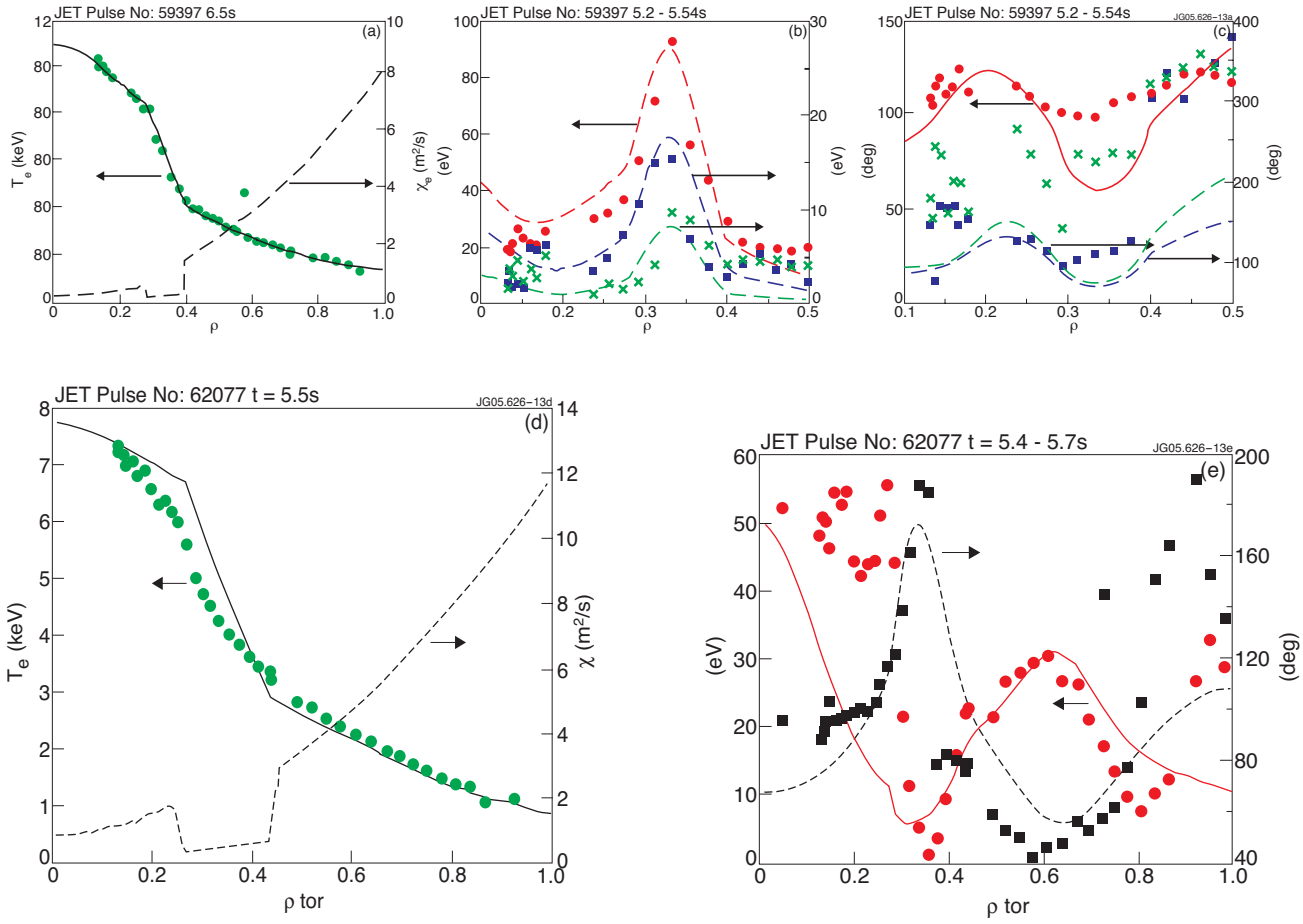

Figure 13 (a): Experimental (circles) and simulated temperature profiles (full line) on the left, compared to the diffusivity adopted in the simulation (dashed line) on the right. (b) First three harmonic amplitudes, simulated vs experimental values. (c) First three harmonic phases, simulated vs experimental values. The reason for the very high values of the experimental phases in Pulse No: 59397 has not been understood yet. (d) Same as a) for Pulse No: 62077 (e) Simulated amplitude and phases versus respective experimental values for Pulse No: 62077. The notation is the one adopted in Figure 12b.

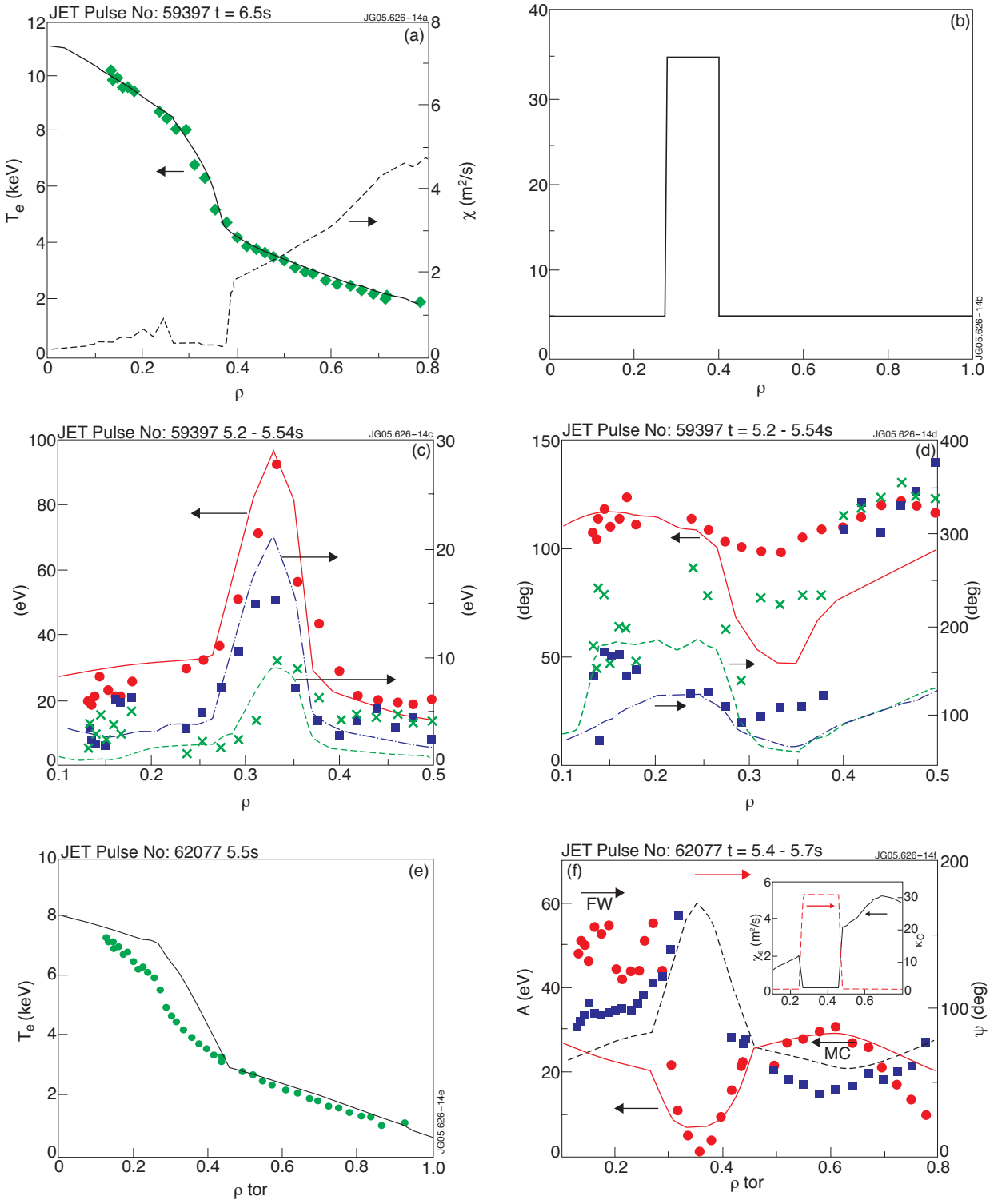

Figure 14 (a): Temperature profiles (exp. and simulated) compared with the χ profile. (b) Threshold adopted in the simulation. c) Simulated versus exp amplitudes of the first three harmonics. (d) First three phases, expressed in degrees. Data refer to Pulse No: 59397. The rapid oscillations in the region 0.15<ρ<0.25 are due to numerical instabilities. By raising the threshold for 0<ρ<0.3, thus stabilizing the whole region bounded by the ITB, it has not been possible to match the temperature profile. (e) Same as (a) for Pulse No: 62077. (f) Experimental (circles) vs simulated (full line) first harmonic amplitude and experimental (squares) versus simulated (dashed line) first harmonic phase for Pulse No: 62077. In the inset figure it is shown the smoothed χ profile versus the threshold used in the simulation. Still numerical instabilities are present in the inner part of plasma. The notation is the one adopted in Figures 13.

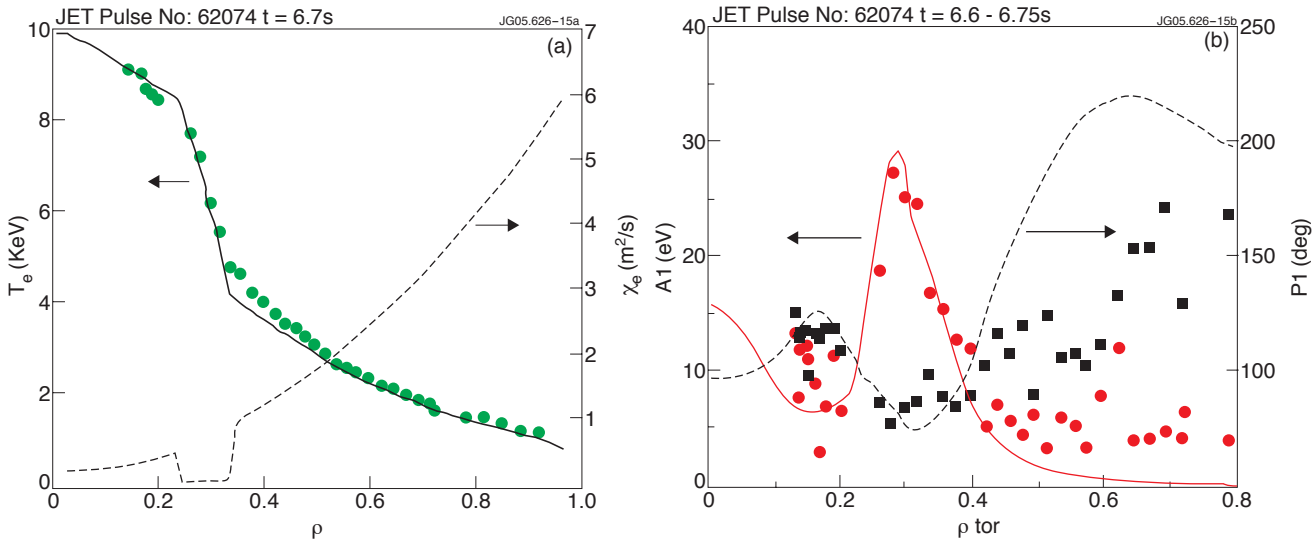

Figure 15 (a): Experimental versus simulated temperature profiles and the χ profile used in the simulation. (b) First harmonic amplitude (full line) and phase (dashed line) simulated versus experimental results (points and squares respectively). Also due to a higher modulation frequency the minimum of the phase is now reproduced in a fair way in the MC deposition region. We note, however, a strong disagreement outside the ITB. Due to the high instability of the plasma for this discharge only the first harmonic is sufficiently free of noise.

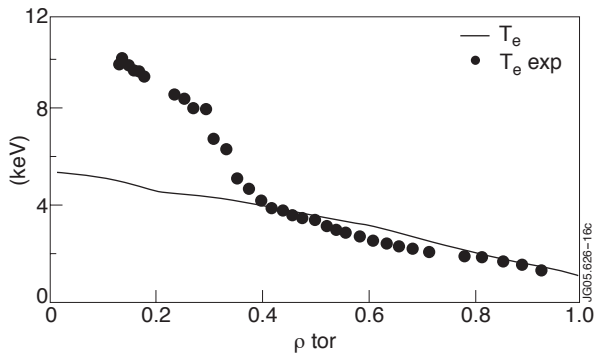

Figure 16: Simulation of the Pulse No: 59397 at t = 6s. using the GLF23 model. Maximum experimental scale lengths at this time are L_{Te} = 10 L_{Ti} = 10 L_{ne} = 2 The simulation does not reproduce the experimental results.